Size and Dynamics of the *Vibrio cholerae* Porins OmpU and OmpT Probed by Polymer Exclusion

Guillaume Duret and Anne H. Delcour*
Department of Biology and Biochemistry, University of Houston, Houston, Texas

ABSTRACT The trimeric OmpU and OmpT porins form large, triple-barrel hydrophilic channels in the outer membrane of the pathogen *Vibrio cholerae*. They have distinct pore properties, such as conductance, block by deoxycholic acid, and sensitivity to acidic pH. Their three-dimensional structures are unknown, but they share significant sequence homologies. To gain insight into the molecular basis for the distinct functional properties of these two similar porins, we carried out polymer exclusion experiments using planar lipid bilayer and patch-clamp electrophysiology. By studying the partitioning of polyethylene glycols (PEGs) of different molecular weights into each porin, we determined an effective radius of 0.55 nm and 0.43 nm for OmpU and OmpT respectively, and found an increased OmpU effective radius at acidic pH. PEGs or high buffer ionic strength promotes the appearance of single step closures in OmpU similar to the acidic-pH induced closures we documented previously. In addition, these closing events can be triggered by nonpenetrating PEGs applied asymmetrically. We believe our results support a model whereby acidic pH, high ionic strength, or exposure to PEGs stabilizes a less conductive state that corresponds to the appearance of an additional resistive element on one side of the OmpU protein and common to the three monomers.

INTRODUCTION

Porins form water-filled β-barrel pores used for the flux of ions and hydrophilic solutes across the outer membrane of Gram negative bacteria, and play an important role for bacterial survival and adaptation toward the changing conditions in the environment. The characterization of these pore-forming proteins by electrophysiological techniques began >30 years ago (1,2), and this experimental approach keeps providing new insights in the molecular properties of porins. Together with crystallography, computer simulations, and mutagenesis, the patch-clamp and planar lipid bilayer techniques have been major contributors to the understanding of permeability, selectivity, and modulatory properties of these nanopores (for review see Delcour (3) and Nikaido (4)).

OmpU and OmpT are the two major porins of the human pathogen *Vibrio cholerae*. They are organized as trimers and, although the actual three-dimensional structures are unknown, each subunit is assumed to contain a pore in the center of the β-barrel, by analogy with the known structures of the OmpF and OmpC porins of *Escherichia coli* (5,6). In vivo, these two porins play an important role in the sensitivity of the bacteria toward bile, and more specifically toward the bile salt deoxycholate (DOC). Cells expressing solely OmpT are less able to survive a DOC-containing environment than cells expressing solely OmpU (7,8), and it was suggested that this might be due to better permeation of DOC through OmpT than OmpU (9). Indeed, we have shown in patch-clamp experiments that OmpT, but not OmpU, can be transiently and reversibly blocked by deoxycholic acid in a concentration range of 20–200 μM (10). As DOC is capable to exert this effect from either side of the membrane, this observation suggests that DOC can translocate through OmpT but not OmpU. A molecular explanation for these results might be that OmpU excludes DOC because of its cation-selectivity, but we showed that the protonated uncharged form of DOC seems to be the effective substrate (10). On the other hand, OmpT might be a larger pore than OmpU to allow passage of DOC, in agreement with the greater antibiotic fluxes measured in vivo for cells expressing OmpT than for cells expressing OmpU (11). But this is in contradiction with early in vivo experiments suggesting that large sugars can translocate through OmpU but not OmpT (12).

OmpU and OmpT have very unique electrophysiological properties. Both porins display a high open probability (Po), and trimeric conductances (g) of 980 pS for OmpU (13) and 1300 pS for OmpT (in 150 mM KCl at pH 7.2). These features are similar to those of the *E. coli* OmpF porin, whose conductance is ~940 pS in the same conditions (14). Contrarily to OmpF and OmpU, OmpT shows a rich kinetic behavior with frequent transient reductions in current corresponding to one third of the open trimeric current and therefore attributed to the closure of a monomer (Fig. 1 *A*). *E. coli* porins are known to be quite sensitive to acidic pH (15–18), and OmpF displays a characteristic kinetic pattern at low pH, whereby open channel noise is increased greatly by rapid flickering to substates whereas the porin slowly reaches a full closed state via the sequential stepwise closure of each of its monomers (15,17). On the other hand, acidic pH produces different behaviors on the *V. cholerae* porins. Acidic pH has a minor effect on OmpT closures (Fig. 1 *A*), with a slight increase in frequency and dwell time at

Submitted October 31, 2009, and accepted for publication January 7, 2010.

*Correspondence: adelcour@uh.edu

Guillaume Duret's present address is Institut Pasteur, Dept. Neuroscience, Groupe Recepteurs Canaux, 25 rue du Dr Roux, 75015 Paris, France.

Editor: Benoit Roux.

0006-3495/10/05/1820/10 $2.00

doi: 10.1016/j.bpj.2010.01.010

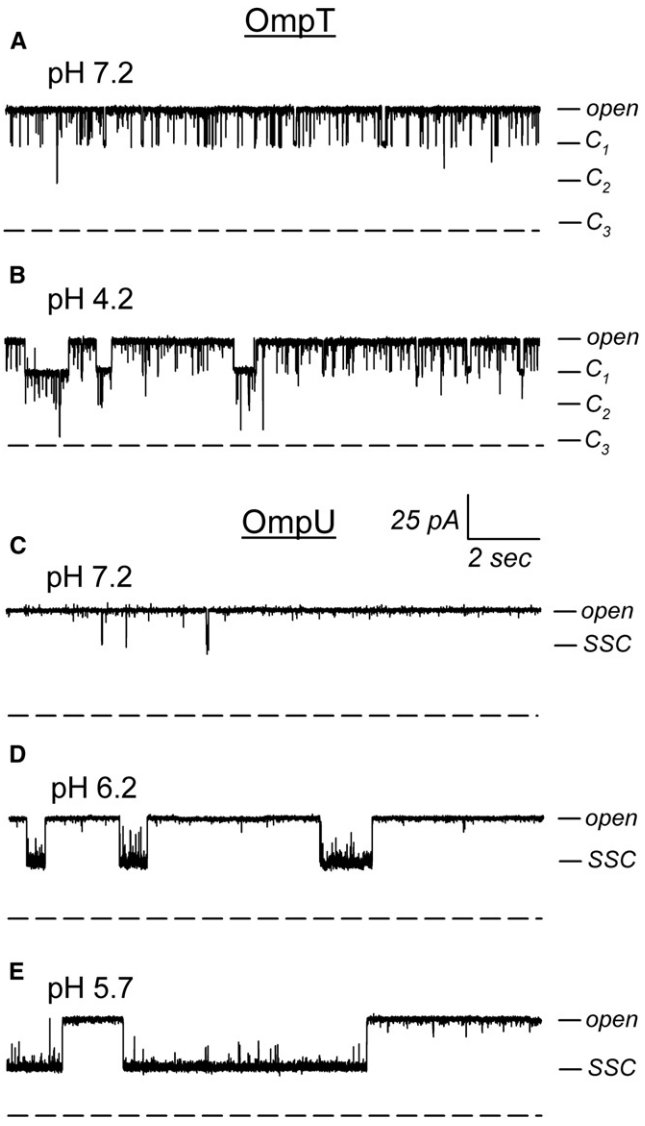

FIGURE 1 Typical behavior of OmpU and OmpT at neutral and acidic pHs. Representative patch-clamp recordings of a (*A* and *B*) single OmpT trimer and (*C–E*) a single OmpU trimer in symmetric conditions of 150 mM KCl in buffer at the indicated pHs. The pipette voltage is +50 mV. The tick mark labeled ''open'' indicates the current level of the fully open trimer; C1, C2, and C3 indicate the levels corresponding to the closures OmpT monomers (*A* and *B*). (*C–E*) Tick mark of labeled SSC indicate the single step closure level observed for OmpU. The dashed line is the 0 pA level. Note the increase in the size of the SSC whereas the full conductance of the open trimer does not vary.

pH 4.2, resulting not in the sequential closure of the three monomers as in OmpF, but rather in the appearance of superimposed closures of two or three monomers, as seen for the patch-clamp traces shown in Fig. 1 *B* (13). On the other hand, as shown in Fig. 1 *C*, OmpU forms quieter pores at neutral pH, with rare transient closing events (19). As for the other porins, the open probability of OmpU is drastically reduced at acidic pHs. However, acidic pH does not induce the appearance of additional closures of the three OmpU monomers, but rather produces an increase in size, duration, and frequency of single step closures (SSCs) only (Fig. 1, *D* and *E*). This peculiar behavior is in sharp contrast to that of OmpT and the *E. coli* porins, and has been witnessed only in OmpU (13). At neutral pH, the size of the SSCs is about one-third of the total conductance, whereas it reaches >50% of the total conductance as the pH is decreased (the traces of Fig. 1 were obtained in patch-clamp in symmetric pH conditions and show a more drastic effect than in asymmetric pH conditions as published previously (13)). This observation alone suggests that the SSCs cannot be due to the sole closure of a monomer. Superimposed closures of multiple monomers are never observed, even when the pH effect is so drastic that the porin seldom dwells at the full trimeric open state.

The effect of DOC on OmpT and the modulation of OmpU by pH raise the question of the actual pore dimensions for these two porins and whether the SSCs truly represent physical pore closures. Nonelectrolyte polymers have been extensively used to measure the volume or diameter of pores (20–25). The most commonly used molecules are the water-soluble uncharged polymers from the polyethylene-glycol (PEG) family, which can be of various sizes. PEGs decrease the macroscopic conductivity of the solution in which they are diluted in a concentration-dependent but size-independent manner (26). Therefore, in an electrophysiological experiment, when the dimensions of the polymer permit full access to the pore lumen, PEGs generate a decrease in pore conductance in the same proportion as they decrease the bulk solution conductivity. On the other hand, conductance remains essentially unchanged for PEGs that are too large to enter the pore. By probing the conductance in the presence of PEGs of different sizes, we can determine the molecular weight cut-off over which the PEGs are excluded from the pore and calculate the pore dimensions. The effective radius of OmpF was successfully determined using this technique and confirmed by the available crystallographic structural data. A molecular weight cut-off of 1360 was determined for OmpF (20), which corresponds to a pore radius of 0.7 nm, similar to the crystallographic pore dimensions of 1.1 by 0.7 nm (6). In addition, polymer exclusion was used to show that the *Streptococcus aureus* α-toxin channel oscillates between states of high- and low-conductance, which are in fact more similar in physical size than anticipated from the conductance ratio, and thus these experiments suggested that the channel does not undergo a physical closure (27).

In this study, we have used polymer exclusion experiments to probe the pore dimensions of the *V. cholerae* OmpU and OmpT porins. The results show the lack of strict correlation between the conductance and pore size measured by polymer exclusion, as OmpT has a lower molecular weight cutoff than OmpU, although its conductance is larger. In addition, the data shed some light on the nature of the acid pH-induced closures of OmpU and suggest that the molecular basis for the spontaneous closing activity is of a different nature for OmpU than for OmpT.

MATERIALS AND METHODS

Chemicals, buffers, and media composition

Luria-Bertani (LB) medium contained 1% tryptone and 0.5% yeast extract (both from Difco; Becton Dickinson, Sparks, MD) and 1% NaCl. *N*-octyl-oligo-oxyethylene (octyl-POE) was purchased from Axxora (San Diego, CA). The pentane and hexadecane used in planar lipid bilayer experiments were from Burdick and Jackson (Honeywell, Muskegon, MI) and TCI America (Portland, OR), respectively. All other chemicals were from Sigma (St. Louis, MO). Electrophysiology buffers always contained 0.1 mM K-EDTA, 10 μM $CaCl_2$ and 5 mM Hepes (pH ranging from 5.7 to 7.2) or 5 mM 2-(*N*-morpholino)ethanesulfonic acid (pH lower than 5.7), and KCl concentrations ranging from 150 mM to 2 M KCl. Therefore, only the KCl concentrations and the pH will be given in the text.

Protein purification

The porins were purified using a protocol described previously (19). Briefly, the proteins were expressed in the porinless *V. cholerae* strain KKV884 (8) from a pBAD30 plasmid carrying the gene of interest behind an arabinose promoter. Cells were grown in LB medium with 0.1 mg/mL of streptomycin and 0.1 mg/mL of ampicillin at 37°C. The expression of porins was induced with 0.01 or 0.05% of L-Arabinose for *ompT* and *ompU* expression, respectively. The cells were harvested at an optical density of 0.6, and lysed by French press (16,000 psi). The membrane fraction was collected at high speed centrifugation (100,000 × g) and resuspended in extraction buffer (10 mM NaCl, 20 mM NaPi, pH 7.6) containing 1% octyl-POE. Consecutive extractions were carried out with 1% and 3% Octyl-POE. The final extract was further purified by ion exchange (Resource Q; GE Healthcare, Piscataway, NJ) and size exclusion (HiLoad 26/20 Superdex 200 prep grade; GE Healthcare) chromatography. The purity and trimeric assembly of the purified porins were confirmed on SDS-PAGE gels with Coomassie Blue staining. We typically obtained a concentration of 0.1–0.7 mg/mL. The aliquoted protein samples were stored at −80°C until used.

Electrophysiology and data analysis

For planar lipid bilayer electrophysiology, a lipid membrane was formed over a 100 μm hole formed in a 0.01 mm Teflon film (Goodfellow, Berwyn, PA) separating two Teflon chambers. The chambers were filled with 1.5 mL of the desired buffer to which 25 μg of lipids (L-α-phosphatidylcholine Type II-S; Sigma,) were added (5 μL of a 5 mg/mL solution of lipids in pentane). The single lipid bilayer membrane was formed by the Montal and Muller technique (28). A total of 5–15 ng of pure protein were added to one side of the membrane only (*cis* side). The insertion of a porin trimer usually occurs within 15 min, as witnessed by a sudden increase in the current on voltage application across the membrane. For each PEG to be tested, 1 g of a 27.27% (w/w) PEG stock solution in the desired buffer was added to each 1.5 mL chamber to give a final concentration of 10.9%. This concentration was purposely used, rather than the typical 15% used in other works (20,29), because we found that higher PEG concentrations enhance the insertions of OmpU in a monomeric form, and make the conductance measurements unreliable. The addition of PEGs to the chambers was carried out from the bottom of the chambers whereas stirring and the final concentrations were checked by conductivity. To remove any trace of PEG and to minimize the insertions of OmpU monomers, the chambers were sonicated in a bath sonicator for 45 min after each experiment.

For patch-clamp electrophysiology, the porins were first reconstituted in artificial liposomes according to a published protocol (30), using the same lipids as for planar lipid bilayer. Unilamellar blisters were induced on the surface of the proteoliposomes in the presence of 20 mM $MgCl_2$ in 150 mM KCl, 0.1 mM K-EDTA, 10 μM $CaCl_2$ and 5 mM Hepes, pH 7.2. Patch pipettes with ~10 megaohm resistance were filled with the appropriate buffer. As the buffer in the pipette cannot be exchanged, the experiments carried out with PEG on both sides of the membrane or with PEG in only the pipette required the pipette to be filled with the buffer containing 10.9% PEG before patching. After patch formation, the buffer of the bath was perfused with the desired solution that did not contain $MgCl_2$.

An Axopatch 1D amplifier connected to a CV-4B (planar lipid bilayer) or a CV-4 headstage (patch-clamp) (Axon Instruments, Foster City, CA) was used to monitor currents under voltage clamp conditions. All voltages given are either on the *cis* side in a bilayer set-up, or pipette voltages in a patch-clamp set-up. The current was filtered at 1 KHz, digitized at 0.1 ms sampling intervals (ITC-18; Instrutech, Port Washington, NY), and stored on a computer using the Acquire software (Bruxton, Seattle, WA). The traces were analyzed by Clampfit (Axon Instruments) and SigmaPlot.

Conductances were consistently measured as the slopes of the linear regressions of the I/V plots of the fully open channel current (trimer) or the SSC current obtained at six different voltages. The cut-off molecular weight (ω_0) for the PEGs was determined by fitting the curve of the conductance ratio $g(\omega)/g_{noPEG}$ versus the molecular weight (ω) to the following equation (20):

$$\frac{g(\omega)}{g_{noPEG}} = (g(\omega)/g_{noPEG})_{max} - \chi \exp(-(\omega/\omega_0)^{\alpha}) \quad (1)$$

where $g(\omega)/g_{noPEG}$ is the ratio of the conductance in the presence of PEGs over the conductance in the absence of PEGs, χ represents the relative amplitude of the conductance of the channel between a regime where PEGs are fully excluded and a regime where they fully enter the pore, α represents the steepness of the transition between the regimes of full exclusion and full inclusion, and ω_o is the cut-off molecular weight for PEG.

For calculation of the effective radius, the following equation was used, according to previous work (20):

$$\left(\frac{\omega_{0(OmpU/T)}}{\omega_{0(OmpF)}}\right)^{0.6} = \frac{r_{OmpU/T}}{r_{OmpF}}, \quad (2)$$

where $\omega_{0(OmpU/T)}$ is the cut-off molecular weight measured for OmpU or OmpT. The cut-off molecular weight measured for OmpF ($\omega_{0(OmpF)}$) is 1360, and the radius (r_{OmpF}) is 0.7 nm from previous work (20). $r_{OmpU/T}$ is the resulting radius calculated for OmpU or OmpT.

RESULTS AND DISCUSSION

OmpU has a larger pore than OmpT

The three-dimensional structures of OmpU and OmpT are unknown. Secondary structure prediction programs suggest that OmpT might have 14 transmembrane β-strands, whereas OmpU is predicted to resemble OmpF with a 16 β-stranded barrel. This might result in a larger pore for OmpU than OmpT. However, the trimeric conductances, as measured from the I/V relationships of the fully open channel current, are 980 pS for OmpU and 1300 pS for OmpT, in 150 mM KCl buffer. These discrepancies prompted us to use polyethylene glycols (PEGs) exclusion experiments in planar lipid bilayer to obtain an independent measurement of the effective radius of the two porins. For each porin insertion, we recorded the current-voltage relationship in the absence and then in the presence of PEGs, at six different voltages. Typical results for OmpU are shown for one voltage in the traces of Fig. 2 *A*, before and after perfusion of a penetrating PEG (MW 200). Note the decrease in the total trimeric current in the presence of the low molecular weight PEG, because of the reduced ion conductivity introduced by

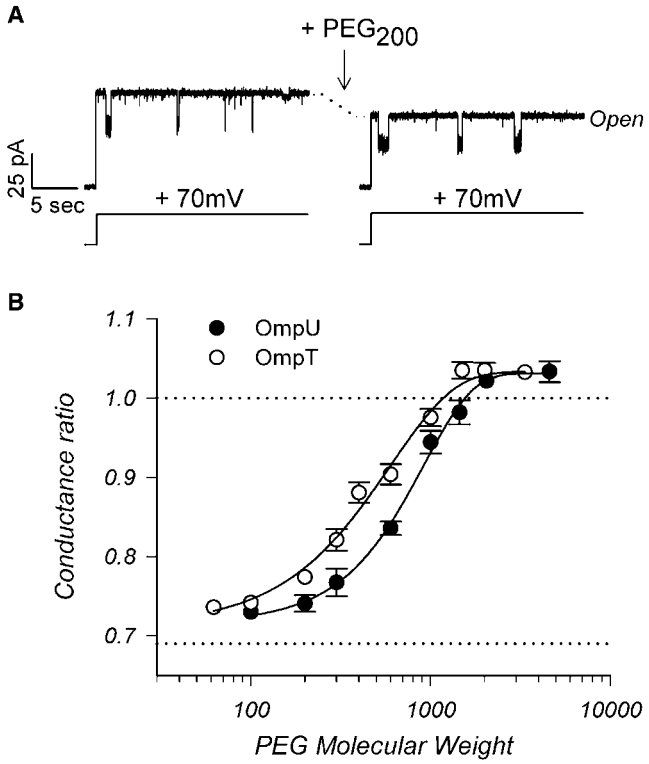

FIGURE 2 OmpU has a larger effective radius than OmpT. (*A*) Effect of penetrating PEGs on the OmpU trimer. The two traces were obtained from the same inserted trimer in planar lipid bilayer (150 mM KCl; pH 7.2), before and after adding PEG200 at a final concentration of 10.9% (w/w). The voltage was stepped from 0 to +70 mV. Note the decrease in the current level corresponding to the fully open trimer (level marked open). (*B*) Molecular weight dependence of the conductance ratio. The conductance ratio is the ratio of the fully open trimer conductance measured in the presence of PEG over the conductance measured without PEGs in the same bilayer. Each data point represents the average conductance ratio measured on two (no error bar) or three or more (error bar) independent experiments. The error bars represent the SE. The data obtained for OmpU (*solid circles*) and OmpT (*open circles*) were fitted to Eq. 1 in Materials and Methods. The molecular weight cut-offs (ω_0) were found to be 916 ± 91 and 598 ± 65 for OmpU and OmpT, respectively. The corresponding effective radius for OmpU and OmpT are 0.55 nm and 0.43 nm, respectively. Other parameters obtained from the fits were: for OmpU: $\chi = 0.31 \pm 0.03$; $\alpha = 1.59 \pm 0.36$; $(\text{conductance ratio})_{max} = 1.03 \pm 0.01$; and for OmpT: $\chi = 0.32 \pm 0.03$; $\alpha = 1.21 \pm 0.24$; $(\text{conductance ratio})_{max} = 1.03 \pm 0.01$.

PEG200 when it resides inside the pore. Similar results were obtained with OmpT.

The conductance was derived from the I/V curve in each PEG condition, and the ratio of the conductances in the presence of PEGs to the absence of PEGs was calculated. This ratio is plotted against the molecular weight of the PEGs in Fig. 2 *B*. The data follow a sigmoidal dependency with a lower plateau close to the expected reduction of bulk electrolyte conductivity due to the presence of PEG at this concentration (0.69, marked by a *dashed line*); as low molecular weight PEGs penetrate in the channel, the conductance scales down proportionally to the decrease in bulk conductivity. The data also converges to an upper plateau slightly ≥ than 1.0 (also marked by a *dashed line*). Here, high molecular weight PEGs are excluded from the channel and the observed small conductance increase is due to the fact that PEG slightly increases ionic activity because of its ability to compete with ions for water binding (25). The observed dependency between the two regimes of penetrating and excluded PEGs is indicative of the interaction of the polymers with the channel, and can be used to derive information on channel size (20,25).

The fit of Eq. 1 to the data yields a molecular weight cutoff of 916 ± 91 for OmpU and 598 ± 65 for OmpT. To determine the corresponding effective pore radius from the molecular weight cut-off, we used the data published by Rostovtseva et al. (20) on the partitioning of PEGs in the OmpF pore. On average, the pores of OmpF permit the entry of PEGs of size ≤1360 Da. This cut-off corresponds to a pore with an effective radius of 0.7 nm, in agreement with crystallographic data (6). Therefore, using Eq. 2 from Materials and Methods, we can calculate the pore of OmpU and OmpT to have an effective radius of 0.55 nm and 0.43 nm, respectively. The justification for the use of equation (2) can be found in Rostovtseva et al. (20) where the authors independently calculated the effective radii of OmpF and the *S. aureus* α-toxin pore and found that the ratio of these effective radii is close to the ratio of the hydrodynamic radii of the cutoff polymer, as determined from curves similar to those shown in Fig. 2 *B*.

Interestingly, we find an inverse correlation between the effective radius and the conductance of the pores. This finding underscores the notion that conductance is not directly related to pore size, but is also influenced by the interactions between channel wall and permeant ions. A similar inverse relationship between conductance and effective radius was reported for OmpF and α-toxin (20), and these authors also cautioned against the use of conductance as a predictor of pore size. In addition, we have reported that mutants in OmpU that have an increased conductance are not necessarily more permeant to large sugars such as maltodextrins, and do not confer an increased sensitivity to antibiotics due to enhanced permeation (31).

The observation that OmpT has a smaller effective radius than OmpU is in agreement with the increased sensitivity of OmpT toward deoxycholic acid relative to OmpU (10). We showed that the protonated form of deoxycholic acid—rather than the anionic form—acts as an open-channel blocker of OmpT at submicellar concentrations. On the other hand, OmpU remains impervious to these concentrations. Based on the results presented above, we believe that the reason for this difference in DOC sensitivity resides in the pore geometries. Indeed, with a smaller effective diameter, we can envision that OmpT provides a tighter fit of the deoxycholic acid molecule in the channel lumen. This in turn would increase the residency time of the deoxycholic acid molecule inside the pore and thus lead to time-resolved blocking events. On the other hand, the less favorable

interactions between a larger OmpU and deoxycholic acid allow the diffusion of DOC with reduced binding. A correlation between the detection of blocking events and binding has also been found for OmpF and various β-lactam antibiotics (32). Note that the presence of a binding site inside the pore lumen facilitates the translocation of the solute through the pore (32). Thus, the smaller effective diameter of OmpT relative to OmpU results in increased affinity of DOC for OmpT and increased translocation. This latter property correlates well with the increased in vivo DOC sensitivity of cells solely expressing OmpT relative to those solely expressing OmpU (7,8).

The effective radius of OmpU is increased by acidic pH

The following experiments on the effect of pH on the effective radius of OmpU were prompted by the observation that the SSCs increase in size at acidic pH (13). We intended to use the same polymer exclusion approach in bilayer to assess the effective radius of OmpU at lower pH. We discovered, however, that the presence of PEG at acidic pH enhanced the insertions of OmpU monomers into the bilayer, making it essentially impossible to get an accurate measurement of the trimeric conductance in these conditions (although we verified that the purified OmpU is trimeric by SDS-PAGE, OmpU is notorious for its sensitivity to disassembly (19), which seems to be enhanced by PEGs). Therefore, we switched to patch-clamp experiments on porins reconstituted into artificial liposomes, where we can limit our study to only those patches that contain a single porin trimer. To mimic the bilayer experiments and avoid complications resulting from asymmetric localizations of PEGs, we carried out the experiments in symmetric conditions of PEG and pH. Because it is not possible to perfuse the pipette, we are not able to compare the results in the presence or the absence of PEGs in the same patch. Rather we are comparing sets of experiments carried out in one or the other condition. For this reason, we are reporting in Fig. 3 the absolute values of the conductance, rather than the conductance ratio, obtained from individual patches.

In general we found that the presence of symmetric acidic pH has a slightly stronger effect than in the asymmetric conditions we reported previously (13); for example, the average duration of the SSCs at symmetric pH of 5.7 in Fig. 1 *E* is ~600 msec, whereas it is ~200 ms in asymmetric pH (pH 7.2 in the pipette and 5.7 in the bath; see Duret et al. (13)). We initially reported that the trimeric conductance remains relatively unchanged when the bath pH only is lowered (13), and this seems to be the case here as well, either in the absence of PEGs (Fig. 3, *white bars*), or in the presence of the excluded PEG4600 (Fig. 3, *black bars*). For an unknown reason, we were not able to observe the expected decrease to 80% in conductance in PEG600 relative to the no-PEG control at pH 7. 2 (compare with Fig. 2 *B*).

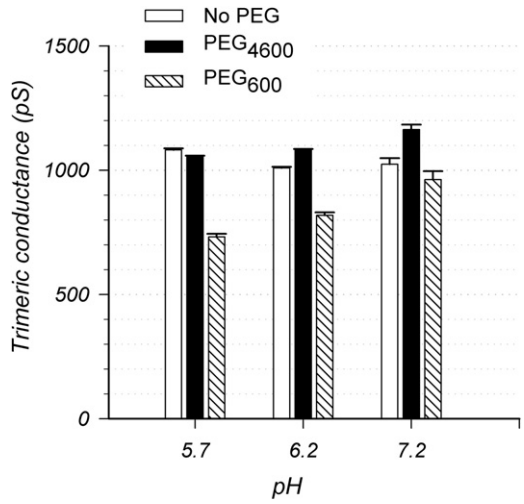

FIGURE 3 The effective radius of OmpU is increased at acidic pH. The conductance of the fully open OmpU trimer was measured in patch-clamp at different symmetric pHs, and in the absence or the presence of a penetrating PEG (PEG600) or a nonpenetrating PEG (PEG4600) applied symmetrically. Each conductance measurement was derived from the current voltage relationship. In the absence of PEGs, the conductance of OmpU is not significantly modified by acidic conditions. The presence of penetrating PEG600 decreases the conductance to a larger extent at lower pH; at pH 5.7, $g_{600}/g_{4600} = 0.69$, which is the lower limit due to the effect of PEGs on conductivity, suggesting that PEG600 can fully enter in the pore.

However, there is an decrease to 80% when the conductance in PEG600 is compared to that in PEG4600. Possibly the microenvironment of the pipette might create artifacts that make it difficult to compare the data with and without PEGs. Thus, in patch-clamp experiments where PEGs are present in the pipette, we have used the condition in nonpenetrating PEG4600 as a control (the conductance in PEG4600 is only 3% higher than in the absence of PEGs in bilayers; see Fig. 2). Importantly, there is a clear and significant decrease in conductance in PEG600 as the pH drops from 7.2 to 5.7 (Fig. 3, *hatched bars*). As PEG600 is situated between the fully excluded and fully penetrating regimes (Fig. 2 *B*), a decrease in conductance in PEG600 is indicative of a progressively better permeation of PEG into the pore, and hence of an increased pore size at lower pH. Indeed, at pH 5.7, the ratio reaches the expected value for a fully penetrating PEG (because it equals the relative conductivity for PEGs at this concentration), indicating that the pore is now wide enough to allow PEG600 to enter completely. We had initially planned to reconstruct a full pH dependence curve, but PEGs seem to enhance the SSCs (see below), such that at pHs <5.7, the combined presence of PEG and low pH leads to a channel that is never in the fully open state, and the measurement of trimeric conductance is not possible.

Nestorovitch et al. (17) carried out similar experiments with OmpF, where they measured the conductance in the presence of PEG1000 over a wide pH range. They found that in the range of pH 4 to 10, there was essentially no

difference in the conductance ratio, suggesting that, for OmpF, the acidic pH modulation of activity is not accompanied by a change in pore size. For OmpU, it seems that the effective radius is somewhat increased at lower pH. Because the effective radius is essentially an average over the length of the channel (20), an increased effective radius value does not necessarily imply that the geometry of solely the constriction zone has changed. We envision that slight modifications in the position of residues along the whole channel wall might be responsible for the observed effect. Whether the change in the size of the SSCs at lower pH has the same basis as for the whole channel remains difficult to ascertain, as we believe that the SSCs represent a phenomenon that is unlinked to the monomeric pores per se (see below).

Nature of the SSCs

The SSCs represent a peculiar phenomenon for porin channels. As shown in Fig. 1 for OmpT and in other publications on *E. coli* porins (14,17), porins typically close in 3 steps that represent the 3 monomers acting as independent channels. Although it is possible to observe the sequential closures of OmpU monomers at high membrane potentials (see Duret et al. (13), and below), the enhanced closing activity at acidic pH is manifested by an increase in frequency and duration of a SSC, as shown in Fig. 1. Similarly, the SSCs are also promoted by increasing the ionic strength of the recording buffer. The traces of Fig. 4, *A–D*, were obtained in symmetric conditions at the indicated KCl concentrations (at pH 7.2). A slight increase in the SSC size and frequency is already observed in 500 mM KCl, but the effect becomes even more pronounced at 1 and 2 M KCl (note the different scale bars for each trace). As observed at more acidic pH, the conductance of the SSC relative to the fully open trimer increases with ionic strength (Fig. 4 *E*), and the SSCs become longer and more frequent, with a concomitant reduction in the average open time of the trimer (Fig. 4 *F*).

Interestingly, PEGs also seem to favor the SSCs. This effect is qualitatively illustrated by the traces of Fig. 5, *A–C*, obtained in symmetric conditions either in the absence of PEGs or in the presence of a penetrating (PEG600) or

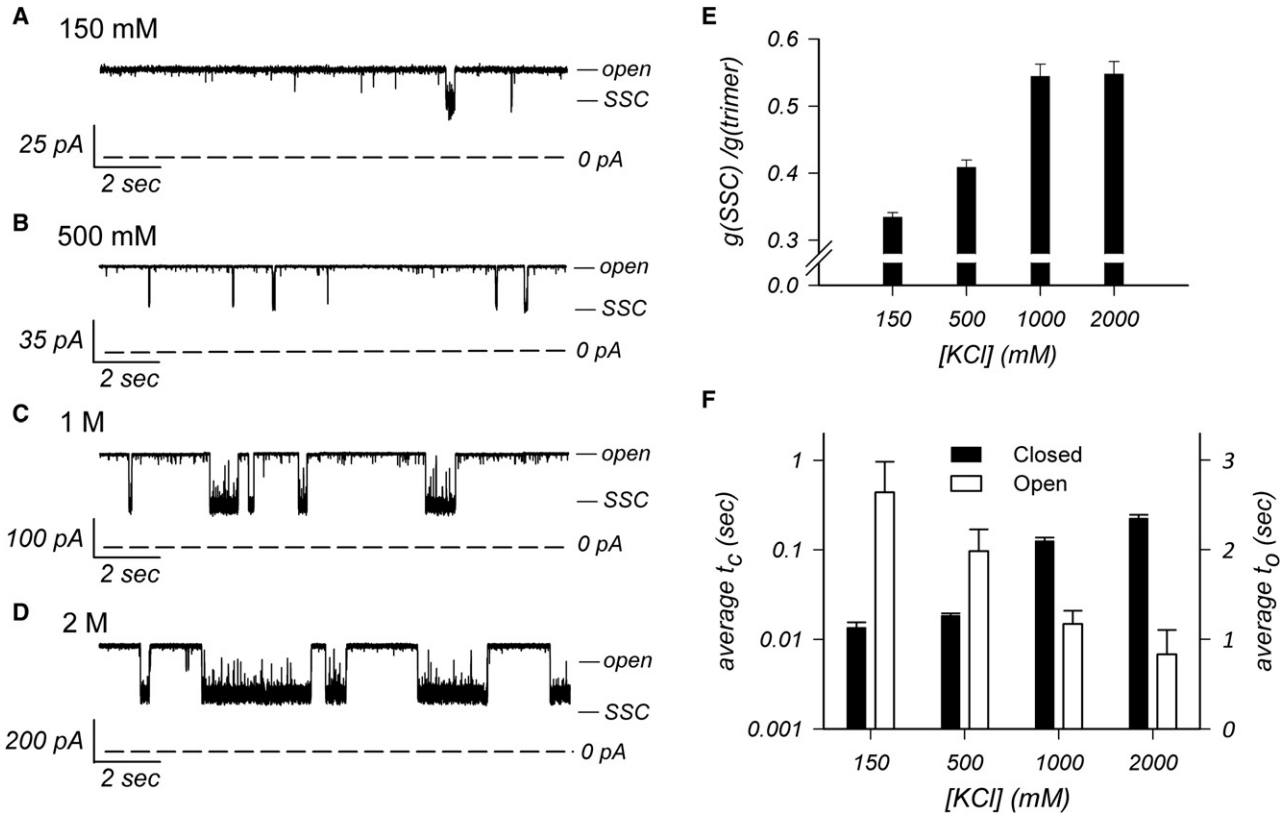

FIGURE 4 Higher ionic strength stabilizes the SSCs. (*A–D*) Representative current traces of OmpU recorded at various symmetric KCl concentrations (pH 7.2), as indicated. The open trimer conductance is increased by higher ionic strength as indicated by the change in scale bar from *A* to *D*. The pipette voltage was +50 mV. Note that the SSCs become larger, longer in duration and more frequent as the buffer ionic strength is increased. (*A*,*C*,*D*) Recorded in planar lipid bilayer. (*B*) Recorded in patch-clamp. (*E*) Plot of the average ratio of SSC conductance (g(SSC)) over the open trimer conductance (g(trimer)) versus KCl concentration in the buffer. Error bars are SE ($n \geq 3$). (*F*) Plot of the average dwell time of the SSC (average t_c; black histogram bars) and of the dwell time of the fully open trimer (average t_o; white histogram bars) versus KCl concentration in the buffer (at pipette voltage of +50 mV). Error bars are SE ($n \geq 3$). Note the logarithmic scale for the left y axis.

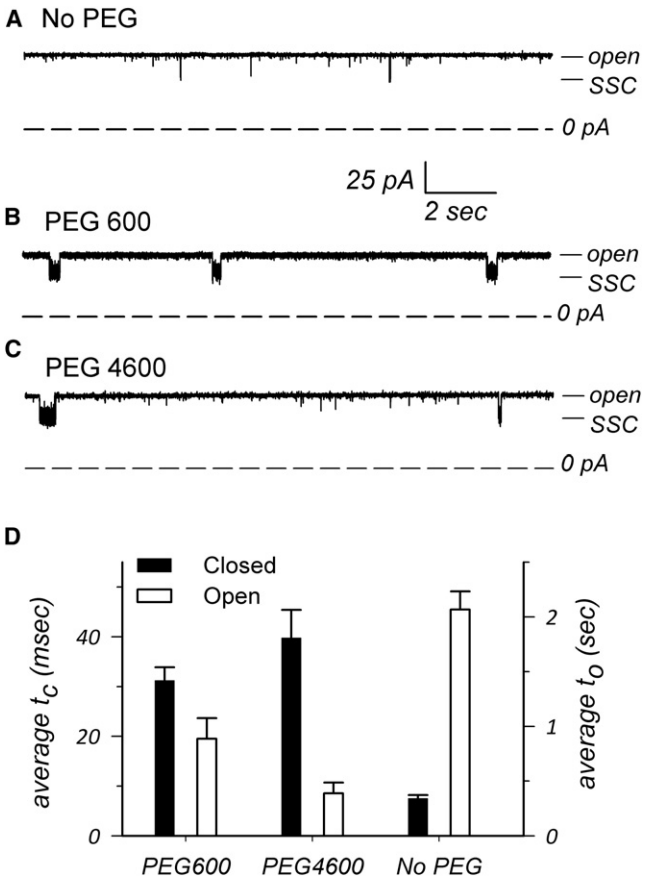

FIGURE 5 The presence of PEGs promotes SSCs. (*A–C*) Representative traces of a single OmpU trimer were recorded in patch-clamp at +50 mV in the (*A*) absence or the (*B*) presence of symmetric penetrating PEG600 or (*C*) nonpenetrating PEG4600 in a 150 mM KCl buffer at pH 7.2. The presence of PEGs on both sides of the membrane triggers longer and more frequent closures. (*D*) Plot of the average dwell time of the SSC (average t_c; black histogram bars) and of the dwell time of the fully open trimer (average t_o; white histogram bars) in the absence or the presence of PEGs, as indicated. Error bars are SE ($n \geq 3$). Pipette voltage is +50 mV.

nonpenetrating (PEG4600) polymer at pH 7.2. Fig. 5 *D* shows the average open time of the trimer and the average closed time of the SSCs in the absence or the presence of PEGs. There does not seem to be a relationship between the size of the PEGs and these parameters; however, we find that the presence of PEGs in general decreases the trimeric open time and increases the SSC dwell time. Note that the effects are less drastic than in the absence of PEG at high ionic strength (Fig. 4 *F*) or at low pH (for example, the average closed time at pH 5.2 (in 150 mM) is >1700 ms (13)). Interestingly, these effects are found regardless of whether PEG penetrates or not the channel, suggesting that the SSC phenomenon may not involve the pores themselves (see below).

Although the structure of OmpU is unknown, we believe it is unlikely that OmpU would be organized as a single pore formed by β-strands contributed by each subunit, in a manner similar to TolC (33). Indeed the high level of homology (25% identity, 40% similarity) between OmpU and OmpF predicts a 16-β-strand motif for OmpU; if each monomer contributed the same number of β-strands, the resulting pore would be extremely large, but the polymer exclusion experiments presented here demonstrate that the OmpU pore has a size cutoff in the range of that of OmpF. Indeed, a modeled OmpU structure very similar to that of OmpF has been presented (34), and it is likely that OmpU is constructed on a triple-barrel motif as other general diffusion porins.

How can we explain a single step closure from a triple barrel protein? If the SSC represents an event occurring at the level of a single monomer (either a physical closure or a reorganization of pore charge distribution leading to a decreased conductance), we would expect the conductance of the SSC to scale proportionally to that of the trimer either in increasing ionic strength conditions, or with more acidic pH. Fig. 4 *E* shows that this is not the case. Although the conductance of the SSC is close to ~1/3 of the trimeric conductance in 150 mM KCl at pH 7.2, it becomes much larger at higher ionic strength, reaching values even greater than 50% in 2 M KCl (pH 7.2). Similarly, the ratio of SSC conductance to the full open trimer conductance is 46% at pH 5.7 (150 mM KCl). Thus these events are unlikely to originate from a single monomer. On very rare occasions, we have obtained traces showing a closing transition of ~1/3 of the trimeric conductance among the dominant SSC events of size >1/3 the trimeric conductance, lending support to the notion that the SSC represents a distinct phenomenon. We have reported previously that OmpU does show a three-step sequential closure of the whole trimer at high voltages, even at low pH, thus supporting the assumption that the protein is indeed organized as a triple barrel (13).

An alternate scenario is that the SSC represents the highly cooperative closure of the three monomers, but with each monomer closing only partially. In this case, we would expect the left-over conductance to have different size exclusion properties from the full open trimeric conductance, in particular to show a reduced effective radius. To probe this, we have analyzed the PEG dependency of the left-over conductance, as shown in Fig. 6 *A*. These experiments were carried out in symmetric PEG conditions in patch-clamp at pH 7.2, and therefore we have normalized the data to the conductance obtained in the presence of the nonpermeating PEG4600, to control for potential artifacts introduced by the presence of PEGs in the pipette. The PEG dependency of conductance ratios for the trimeric conductance (Fig. 6, *gray circles*) and the left-over conductance (Fig. 6, *black circles*) is found to match the dependence obtained for the trimeric conductance in bilayer experiments (Fig. 6, *dashed line*, is the fit of the OmpU data in Fig. 2 *B*, normalized to the PEG4600 fitted value). Therefore, the left-over conductance does not originate from partially closed monomers. Even if the pores spontaneously reorganize the charge constellation at the constriction zone to lead to a decreased conductance by electrostatic effects (without

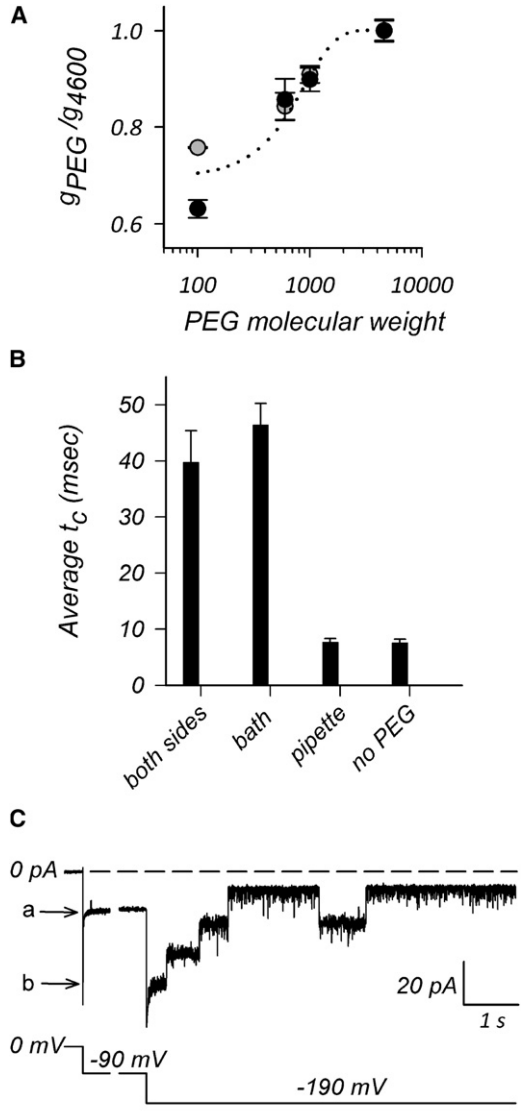

FIGURE 6 The SSCs do not involve the pores per se. (*A*) Plot of conductance ratios versus PEG molecular weight. The conductances were obtained from three or more independent experiments in patch-clamp (150 mM KCl; pH 7.2), and normalized to the average conductance measured for a fully excluded PEG (PEG_{4600}) to control for potential artifacts due to the presence of PEGs in the pipette. Experiments were carried out in patch-clamp to prevent insertions of monomers, which often occur in bilayers when PEGs are present. Dark circles represent the ratio of the left-over conductance during an SSC, and gray circles are the ratio of the fully open trimer conductance. The dotted line represents the fit obtained from bilayer data on OmpU from Fig. 2 *B*, normalized to the excluded-PEG conductance ratio. (*B*) Plot of the average dwell time of the SSCs (average t_c) in the presence or absence of nonpenetrating PEG4600 in buffer with 150 mM KCl (pH 7.2) at a pipette voltage of +50 mV. The error bars are SE ($n \geq 3$). Whether PEG4600 is present on both sides of the patch, or only on the pipette side or the bath side is indicated. (*C*) Patch-clamp trace of a single trimer of OmpU obtained in the presence of symmetric PEG100 in 150 mM KCl buffer at pH 6.2. The cumulative effect of PEG100 and pH 6.2 leads to a stable SSC state (current level at −90 mV marked by letter a). The voltage was then switched to −190 mV in the hope of reopening the channel, but this did not occur and the channel remained in the SSC state (current level at −190 mV marked by letter b). The high voltage, however, triggered the voltage-dependent inactivation of the porin (13) in three consecutive steps representing the sequential closure of each pore of the trimer.

physical reduction of the pore diameter) during an SSC, it would be extremely unlikely, and hard to conceive, that this pore-specific event occurred precisely at the same time for all three pores.

A final scenario is that the SSC is an epiphenomenon that does not involve the pores per se, but perhaps corresponds to the transient introduction of an additional resistance that affects all three pores simultaneously. The PEG dependency of the left-over conductance supports the idea that the effective radius of the pores has been left unchanged during the SSC. We envision that the SSC might represent a transient conformational change that affects all three pores simultaneously, for example at the level of extracellular loops. Possibly, these loops might close over the trimer and form a kind of antechamber or vestibule that limits the access of ions to the pores themselves. Because PEGs enhance SSCs, we reasoned that a nonpenetrating PEG should promote the SSCs in an asymmetric manner if indeed the SSCs are due to events occurring at the surface of the channel, such as at the level of the loops. Thus we compared the average dwell time of the SSCs in the absence of PEG4600 or in the presence of PEG4600 on either side of the patch and on both sides of the patch. The results of Fig. 6 *B* show that the SSCs remain extremely short when PEG4600 is in the pipette only, as in the absence of PEG, i.e., PEG4600 is ineffective when applied in the pipette only. However, the average dwell time of the SSCs when PEG4600 is in the bath only is comparable to the value obtained when PEG4600 is present on both sides. Thus, the presence of nonpermeating PEGs on the bath-side of the patch does lead to a stabilization of the SSC. These results are highly suggestive that the SSCs originate from events that occur on one side only of the channel.

This scenario would not hamper the individual monomers from undergoing the typical three-step closure observed at high voltages due to voltage-dependent inactivation (13), as shown in Fig. 6 *C*. Here the patch was bathed in symmetric pH 6.2 in the presence of PEG100, promoting a stable SSC at −90 mV (level marked by letter a) due to the combination of PEG and acidic pH. On switching the voltage to −190 mV, the current jumps to the corresponding SSC current at this voltage (marked by letter b; the fully open trimeric current at this voltage would be −180 pA); within <1 s, this event is followed by three sequential closures, most likely representing that of the three monomers. This type of behavior underscores the notion that the SSC does not correspond to the closure or modification of a single monomer of the trimer.

We envision that the reduced conductance of the trimer during an SSC is the result of a spontaneous modification of the architecture of the trimer in a region that encompasses the three pores altogether and leads to a reduced access of permeant ions to the pore entries. Such a scenario has been

also proposed by Gurnev et al. (35) for the conductance changes observed on binding of phage λ to LamB. Because we do not know the orientation of the channel, we cannot ascertain that this region does indeed correspond to the extracellular loops. However, we favor the hypothesis of the involvement of the loops because the extracellular loops have been implicated in the pH-dependent modulation of OmpF activity (15). Confirmation of this hypothesis would require further experimentation on loop mutants.

The extracellular loops might oscillate back and forth, occasionally partially obstructing the entry of ions into the pores, and thus triggering an SSC. At acidic pH, higher ionic strength or in the presence of PEGs, the obstruction is not only favored and stabilized—leading to changes in the kinetics of the SSCs—but also more embracing, resulting in a more extensive conductance decrease relative to the trimer size. In the absence of any structural model, it is difficult to propose a molecular scenario for this phenomenon. Our results suggest that the presumed conformational changes that lead to the SSC and the extent of the conductance decrease during this event are sensitive to the electrostatic profile of the channel. Protonation of acidic groups or increase in bulk ionic strength have the effect of diminishing the impact of charged residues on channel conformation. Similarly, PEGs are known to compete with ions for water binding, leading to an increase in ion activities (25). Thus, PEGs might also reorganize water around key residues on the channel, mimicking the effect of protonation or charge shielding at these precise locations. We previously documented that both the average SSC dwell time and the average time in between SSCs (i.e., open time of the trimer) are pH-dependent (13). This would not be the case if the entry into and exit from a SSC corresponded to a protonation-deprotonation event. Rather, we believe that the protonation state of the protein modulates the kinetics of the SSC, itself representing an intrinsic spontaneous oscillation between two OmpU conformations.

This work was supported by the Welch Foundation (E-1597).

REFERENCES

1. Benz, R., K. Janko, …, P. Läuger. 1978. Formation of large, ion-permeable membrane channels by the matrix protein (porin) of *Escherichia coli*. *Biochim. Biophys. Acta.* 511:305–319.
2. Schindler, H., and J. P. Rosenbusch. 1978. Matrix protein from *Escherichia coli* outer membranes forms voltage-controlled channels in lipid bilayers. *Proc. Natl. Acad. Sci. USA.* 75:3751–3755.
3. Delcour, A. H. 2003. Solute uptake through general porins. *Front. Biosci.* 8:d1055–d1071.
4. Nikaido, H. 2003. Molecular basis of bacterial outer membrane permeability revisited. *Microbiol. Mol. Biol. Rev.* 67:593–656.
5. Baslé, A., G. Rummel, …, T. Schirmer. 2006. Crystal structure of osmoporin OmpC from *E. coli* at 2.0 Å. *J. Mol. Biol.* 362:933–942.
6. Cowan, S. W., T. Schirmer, …, J. P. Rosenbusch. 1992. Crystal structures explain functional properties of two *E. coli* porins. *Nature.* 358:727–733.
7. Provenzano, D., and K. E. Klose. 2000. Altered expression of the ToxR-regulated porins OmpU and OmpT diminishes *Vibrio cholerae* bile resistance, virulence factor expression, and intestinal colonization. *Proc. Natl. Acad. Sci. USA.* 97:10220–10224.
8. Provenzano, D., C. M. Lauriano, and K. E. Klose. 2001. Characterization of the role of the ToxR-modulated outer membrane porins OmpU and OmpT in *Vibrio cholerae* virulence. *J. Bacteriol.* 183: 3652–3662.
9. Klose, K. E. 2001. Regulation of virulence in *Vibrio cholerae*. *Int. J. Med. Microbiol.* 291:81–88.
10. Duret, G., and A. H. Delcour. 2006. Deoxycholic acid blocks *Vibrio cholerae* OmpT but not OmpU porin. *J. Biol. Chem.* 281: 19899–19905.
11. Wibbenmeyer, J. A., D. Provenzano, …, A. H. Delcour. 2002. *Vibrio cholerae* OmpU and OmpT porins are differentially affected by bile. *Infect. Immun.* 70:121–126.
12. Chakrabarti, S. R., K. Chaudhuri, …, J. Das. 1996. Porins of *Vibrio cholerae*: purification and characterization of OmpU. *J. Bacteriol.* 178:524–530.
13. Duret, G., V. Simonet, and A. H. Delcour. 2007. Modulation of *Vibrio cholerae* porin function by acidic pH. *Channels (Austin).* 1:70–79.
14. Baslé, A., R. Iyer, and A. H. Delcour. 2004. Subconductance states in OmpF gating. *Biochim. Biophys. Acta.* 1664:100–107.
15. Baslé, A., R. Qutub, …, A. H. Delcour. 2004. Deletions of single extracellular loops affect pH sensitivity, but not voltage dependence, of the *Escherichia coli* porin OmpF. *Protein Eng. Des. Sel.* 17:665–672.
16. Liu, N., and A. H. Delcour. 1998. Inhibitory effect of acidic pH on OmpC porin: wild-type and mutant studies. *FEBS Lett.* 434:160–164.
17. Nestorovich, E. M., T. K. Rostovtseva, and S. M. Bezrukov. 2003. Residue ionization and ion transport through OmpF channels. *Biophys. J.* 85:3718–3729.
18. Todt, J. C., W. J. Rocque, and E. J. McGroarty. 1992. Effects of pH on bacterial porin function. *Biochemistry.* 31:10471–10478.
19. Simonet, V. C., A. Baslé, …, A. H. Delcour. 2003. The *Vibrio cholerae* porins OmpU and OmpT have distinct channel properties. *J. Biol. Chem.* 278:17539–17545.
20. Rostovtseva, T. K., E. M. Nestorovich, and S. M. Bezrukov. 2002. Partitioning of differently sized poly(ethylene glycol)s into OmpF porin. *Biophys. J.* 82:160–169.
21. Vodyanoy, I., and S. M. Bezrukov. 1992. Sizing of an ion pore by access resistance measurements. *Biophys. J.* 62:10–11.
22. Movileanu, L., and H. Bayley. 2001. Partitioning of a polymer into a nanoscopic protein pore obeys a simple scaling law. *Proc. Natl. Acad. Sci. USA.* 98:10137–10141.
23. Merzlyak, P. G., L. N. Yuldasheva, …, S. M. Bezrukov. 1999. Polymeric nonelectrolytes to probe pore geometry: application to the alpha-toxin transmembrane channel. *Biophys. J.* 77:3023–3033.
24. Carneiro, C. M., P. G. Merzlyak, …, O. V. Krasilnikov. 2003. Probing the volume changes during voltage gating of Porin 31BM channel with nonelectrolyte polymers. *Biochim. Biophys. Acta.* 1612:144–153.
25. Bezrukov, S. M., and I. Vodyanoy. 1993. Probing alamethicin channels with water-soluble polymers. Effect on conductance of channel states. *Biophys. J.* 64:16–25.
26. Stojilkovic, K. S., A. M. Berezhkovskii, …, S. M. Bezrukov. 2003. Conductivity and microviscosity of electrolyte solutions containing polyethylene glycols. *J. Chem. Phys.* 119:6973–6978.
27. Korchev, Y. E., C. L. Bashford, …, C. A. Pasternak. 1995. Low conductance states of a single ion channel are not 'closed'. *J. Membr. Biol.* 147:233–239.
28. Montal, M., and P. Mueller. 1972. Formation of bimolecular membranes from lipid monolayers and a study of their electrical properties. *Proc. Natl. Acad. Sci. USA.* 69:3561–3566.
29. Nestorovich, E. M., E. Sugawara, …, S. M. Bezrukov. 2006. *Pseudomonas aeruginosa* porin OprF: properties of the channel. *J. Biol. Chem.* 281:16230–16237.

30. Delcour, A. H., B. Martinac, …, C. Kung. 1989. Modified reconstitution method used in patch-clamp studies of *Escherichia coli* ion channels. *Biophys. J.* 56:631–636.

31. Lauman, B., M. Pagel, and A. H. Delcour. 2008. Altered pore properties and kinetic changes in mutants of the *Vibrio cholerae* porin OmpU. *Mol. Membr. Biol.* 25:498–505.

32. Danelon, C., E. M. Nestorovich, …, S. M. Bezrukov. 2006. Interaction of zwitterionic penicillins with the OmpF channel facilitates their translocation. *Biophys. J.* 90:1617–1627.

33. Koronakis, V., A. Sharff, …, C. Hughes. 2000. Crystal structure of the bacterial membrane protein TolC central to multidrug efflux and protein export. *Nature.* 405:914–919.

34. Pagel, M., V. Simonet, …, A. H. Delcour. 2007. Phenotypic characterization of pore mutants of the *Vibrio cholerae* porin OmpU. *J. Bacteriol.* 189:8593–8600.

35. Gurnev, P. A., A. B. Oppenheim, …, S. M. Bezrukov. 2006. Docking of a single phage lambda to its membrane receptor maltoporin as a time-resolved event. *J. Mol. Biol.* 359:1447–1455.